

Nonindependent K⁺ Movement through the Pore in IRK1 Potassium Channels

PER STAMPE, JORGE ARREOLA, PATRICIA PÉREZ-CORNEJO, and TED BEGENISICH

From the Department of Pharmacology and Physiology, University of Rochester Medical Center, Rochester, New York 14642

ABSTRACT We measured unidirectional K⁺ in- and efflux through an inward rectifier K channel (IRK1) expressed in *Xenopus* oocytes. The ratio of these unidirectional fluxes differed significantly from expectations based on independent ion movement. In an extracellular solution with a K⁺ concentration of 25 mM, the data were described by a Ussing flux-ratio exponent, n' , of ~ 2.2 and was constant over a voltage range from -50 to -25 mV. This result indicates that the pore of IRK1 channels may be simultaneously occupied by at least three ions. The IRK1 n' value of 2.2 is significantly smaller than the value of 3.5 obtained for *Shaker* K channels under identical conditions. To determine if other permeation properties that reflect multi-ion behavior differed between these two channel types, we measured the conductance (at 0 mV) of single IRK1 channels as a function of symmetrical K⁺ concentration. The conductance could be fit by a saturating hyperbola with a half-saturation K⁺ activity of 40 mM, substantially less than the reported value of 300 mM for *Shaker* K channels. We investigated the ability of simple permeation models based on absolute reaction rate theory to simulate IRK1 current-voltage, conductance, and flux-ratio data. Certain classes of four-barrier, three-site permeation models are inconsistent with the data, but models with high lateral barriers and a deep central well were able to account for the flux-ratio and single channel data. We conclude that while the pore in IRK1 and *Shaker* channels share important similarities, including K⁺ selectivity and multi-ion occupancy, they differ in other properties, including the sensitivity of pore conductance to K⁺ concentration, and may differ in the number of K⁺ ions that can simultaneously occupy the pore: IRK1 channels may contain three ions, but the pore in *Shaker* channels can accommodate four or more ions.

KEY WORDS: ion permeation • unidirectional flux-ratio • single channel conductance

INTRODUCTION

The permeation properties of K channels are quite complex and are not consistent with the independent movement of ions through simple aqueous pores. Rather, these complex properties suggest that the channel pore may simultaneously be occupied by several ions. Some of the properties of ion channels that are consistent with multi-ion pore occupancy include: (a) an apparent concentration-dependent ion selectivity, (b) a voltage sensitivity of pore block by ions that depends on the concentration of the permeant ion or the blocking ion (or both), (c) pore current (or conductance or permeability ratio) that is a nonmonotonic function of the mole fraction of two types of ions (the so-called "anomalous mole-fraction effect"), and (d) deviations from the Ussing (1949) flux ratio test for independent ion movement.

This latter test, as applied by Hodgkin and Keynes (1955), relies on a modified form of the Ussing flux ratio test for independent ion movement:

$$\frac{m_e}{m_i} = \left[\frac{[K]_i}{[K]_o} \exp\left(\frac{V_m F}{RT}\right) \right]^{n'}, \quad (1)$$

where m_e and m_i are unidirectional K⁺ efflux and influx, respectively, $[K]_i$ and $[K]_o$ are the intracellular and extracellular K⁺ concentrations, V_m is the membrane voltage, and R , T , and F have their usual thermodynamic meanings. The flux-ratio exponent, n' , is 1 for a pore in which ion movements are independent; that is, a pore that never contains more than a single ion.

The flux-ratio test has been applied to several types of K channels in native cells, including delayed rectifier channels in cephalopod axons (Hodgkin and Keynes, 1955; Begenisich and De Weer, 1980), the Ca²⁺-activated K channel in erythrocytes (Vestergaard-Bogind et al., 1985), and the inward rectifier K channel in skeletal muscle (Horowicz et al., 1968; Spalding et al., 1981). In all these cases, the flux-ratio exponent was found to be significantly >1.0 , demonstrating the multi-ion nature of these types of channels.

We recently determined the flux-ratio exponent for cloned *Shaker* K channels expressed in *Xenopus* oocytes (Stampe and Begenisich, 1996). We found a value of ~ 3.5 at -30 mV, which is essentially the same as that from native squid axon K channels (Begenisich and De Weer, 1980). The largest n' value for native inward-rec-

Address correspondence to Ted Begenisich, Department of Pharmacology & Physiology, Box 711, University of Rochester Medical Center, Rochester, NY 14642. Fax: 716-244-9283; E-mail: tbb@crocus.medicine.rochester.edu

tifier K channels is ~ 2 (Horowicz et al., 1968; Spalding et al., 1981), considerably less than the values for native and expressed voltage-gated K channels.

To determine if these different n' values for voltage-gated and inward-rectifier K (IRK1)¹ channels represent fundamental differences in the permeation properties of these two types of channels or result from methodological differences, we determined flux-ratio exponents for IRK1 channels with conditions identical to those used for *Shaker* K channels (Stampe and Begegnisich, 1996). We found a constant n' value near 2.2 over the potential range from -25 to -50 mV, which is significantly smaller than the *Shaker* value of ~ 3.5 .

To determine if other permeation properties that reflect multi-ion behavior differed between these two channel types, we measured the conductance (at 0 mV) of single IRK1 channels as a function of symmetrical K⁺ concentration. The conductance could be fit by a saturating hyperbola with a half-saturation K⁺ activity of 40 mM, generally similar to that observed for the weak inward rectifier channel ROMK1 (Lu and MacKinnon, 1994), but substantially less than the reported value of 300 mM for *Shaker* K channels (Heginbotham and MacKinnon, 1993). We found that a simple four-barrier, three-site permeation model can account for the IRK1 flux ratio, as well as the single channel current-voltage and conductance data.

METHODS

Oocyte Preparation

Stage V and VI *Xenopus* oocytes were isolated by methods similar to those described by Goldin (1992). Oocytes were manually defolliculated after a 90-min incubation in 2 mg/ml collagenase Type 1A (Sigma Chemical Co., St. Louis, MO) in Ca-free OR-2 solution (82.5 mM NaCl, 2.5 mM KCl, 1 mM MgCl₂, and 5 mM HEPES, pH 7.6 with NaOH) and maintained at 18°C in ND-96 (96 mM NaCl, 2 mM KCl, 1.8 mM CaCl₂, 1 mM MgCl₂, 5 mM HEPES, and 2.5 mM Na-pyruvate, pH 7.6 with NaOH). Oocytes were injected with mRNA transcribed (T3 mMessage mMachine; Ambion Inc., Austin, TX) from IRK1 (Kir2.1) channel cDNA (Kubo et al., 1993), subcloned into a modified pBluescript vector containing the 5' and 3' untranslated regions of the *Xenopus* globin gene. Oocytes used for unidirectional flux measurements were injected with 0.5 to 1.5 ng of mRNA. Oocytes used for single channel current measurements were injected with 0.16 to 0.5 ng of mRNA. The vitelline membrane was removed before patch clamp recordings.

Two-Microelectrode Voltage Clamp

The experiments in which we measured unidirectional fluxes were done with a custom two-microelectrode voltage clamp system (see Stampe and Begegnisich, 1996, 1998 for additional details). The clamp design included a high output voltage (± 150 V)

amplifier and provision for series resistance compensation. As a result of the inward rectification properties of IRK1 channels, uncompensated series resistance errors were negligible at the more depolarized potentials used in this study (-25 and -30 mV) and <1 mV at the most negative potential (-50 mV). To minimize electrical coupling between the two microelectrodes, the current-passing electrode was coated with a (grounded) conducting paint layer and a second insulating coating. Both electrodes were filled with 3 M KCl and had resistances typically between 0.3 and 0.5 M Ω . The ionic currents are shown (see Fig. 1) without correction for leak or capacity currents. All measurements were made at room temperature (22–24°C).

Single Channel Measurements

We measured single IRK1 channel currents from inside-out patches excised from oocytes 3–5 d after mRNA injection. These currents were obtained with an Axopatch 1D amplifier (Axon Instruments, Foster City, CA). Patch electrodes (typically 5–12 M Ω) were pulled from Corning 7052 glass and coated with Sylgard (Dow Corning Corp., Indianapolis, IN). Patches selected for analysis exhibited inward but not outward currents before excision, consistent with IRK1 channel properties (Kubo et al., 1993). To minimize inhibition of outward current by any residual polyamines (Ficker et al., 1994; Lopatin et al., 1994), voltage steps to positive potentials were made from a negative voltage (usually -80 mV). At K concentrations >200 mM, we observed a fast “flickery” channel (which was also present in uninjected oocytes), but these were readily distinguished from IRK1 channels by their very different kinetic properties. The recordings were made at room temperature (22–24°C).

Solutions

The external (bath) solution used for the unidirectional flux measurements consisted of (mM): 25 KCl, 75 NaCl, 5 MgCl₂, 10 HEPES, pH 7.4. The ⁴²K (2 mCi/mM) was obtained from the Research Reactor Facility at the University of Missouri (Columbia, MO).

The external (pipette) solution for single channel measurements consisted of (mM): 1 MgCl₂, 0.3 CaCl₂, 10 HEPES, pH 7.1, and 50, 100, 200, 300, or 400 KCl. The internal solution consisted of (mM): 5 EGTA, 5 EDTA, 10 HEPES, pH 7.4, and 50, 100, 200, 300, or 400 KCl. We also recorded single channel currents in similar 25 mM K solutions but with 75 mM *N*-methyl-D-glucamine. Some single channel currents measurements were done in Cl⁻ free solutions with methanesulfonic acid as the replacement anion. We were unable to obtain single IRK1 channel activity at K concentrations >400 mM due to a decreased probability of seal formation and the lack of active channels in those patches with good seals (Heginbotham and MacKinnon, 1993).

Unidirectional Fluxes and the Flux-Ratio Exponent

The flux-ratio exponent, n' , was computed from a rearranged form of Eq. 1:

$$n' = \frac{RT}{(V_m - V_K) F} \ln \frac{m_e}{m_i} \quad (2)$$

The determination of n' from Eq. 2 requires values for both unidirectional influx and efflux. As in previous work, we did not measure both fluxes from the same oocyte. Rather, we measured one unidirectional flux and the time integral of ion current (net flux), and computed the remaining unidirectional flux through the following equation:

$$I_{\text{Net}} = F(m_e - m_i) \quad (3)$$

¹Abbreviation used in this paper: IRK1, inward rectifier K channel.

These are called the efflux and influx methods (Begenisich and De Weer, 1980; Stampe and Begenisich, 1996) according to the unidirectional flux that is directly measured. The unidirectional fluxes were obtained from gamma counting (Gamma 4000; Beckman Instruments, Inc., Brea, CA) of trace amounts of ^{42}K .

For measurements of unidirectional influx, the oocyte was placed in a low (75 μl) volume chamber and voltage clamped in the external solution without radiotracer. We used a holding potential (+20 mV) at which most of the IRK1 channels are blocked by internal polyamines and Mg^{2+} ions (Ficker et al., 1994; Lopatin et al., 1994; Yang et al., 1995). The oocyte was allowed a period of time to recover from the electrode impalements. A radiolabeled solution was then introduced into the chamber and for 4 min the membrane potential was stepped (for 300 ms at 1 Hz) to -25, -30, or -50 mV. The oocyte was then rapidly and extensively washed with the external solution without radiotracer with the membrane voltage maintained at +20 mV. The oocyte was then unclamped, the electrodes removed, and the amount of ^{42}K in the oocyte was determined.

To determine the amount of ^{42}K radioactivity not associated with influx through IRK1 channels, we measured ^{42}K influx in (a) oocytes injected with IRK1 RNA and maintained only at the +20 mV holding potential for 4–6 min, (b) oocytes not injected with RNA but subjected to the same voltage protocol as injected cells, and (c) uninjected oocytes maintained at the +20-mV holding potential but without pulsing. As with similar experiments with *Shaker* K channels (Stampe and Begenisich, 1996), there were no significant differences among these three groups of oocytes and the computed influx was linearly related to the ^{42}K -specific activity. This relationship was then used to correct each influx experiment for the amount of radioactivity not associated with influx through IRK1 channels.

For the efflux method, the oocytes were loaded with ^{42}K by soaking them for 8–12 h in a high specific activity solution. After a thorough wash, the oocyte was transferred to the experimental chamber. The external solution was perfused at 1 ml/min by peristaltic pumps and the outflow routed to a fraction collector. 1-min samples were collected for counting of ^{42}K . Unidirectional ^{42}K efflux was obtained at a constant holding potential of -25 mV; the unidirectional influx was computed by subtraction of the measured efflux and the time integral of channel current.

The short half-life of the isotope makes it unrealistic to wait for equilibrium to occur between ^{42}K in the soaking solution and the oocytes. We obtained the specific activity of the internal ^{42}K solution by counting each oocyte at the end of the experiment and determining the internal K^+ content by flame photometry (IL343; Instrumentation Laboratories, Lexington, MA). Oocytes were rapidly washed in a K^+ -free solution (100 mM *N*-methyl-D-glucamine/HCl, 5 mM MgCl_2 , 10 mM HEPES, pH 7.4), and subsequently disintegrated by vortexing in LiCl. The average K^+ content for the oocytes for which ^{42}K efflux was determined was 79 ± 4.7 nmol (\pm SEM, $n = 4$). The diameter of Stage V and VI oocytes is generally between 1.0 and 1.3 mm; for a 1.1-mm-diameter oocyte, this K content would represent an internal K concentration of 118 mM.

Determination of K^+ equilibrium potential. The determination of the flux-ratio exponent from Eq. 2 requires the value of the K^+ equilibrium potential, V_K , which we obtained from the IRK1 channel zero current potential (described in detail below, see Fig. 1). We found an average V_K value of -38 ± 0.7 mV ($n = 17$) with a range of -47 to -32.5 mV. The mean value corresponds to an internal K concentration (ignoring any difference between internal and external K activity coefficients) of 115 mM, quite similar to the estimate above from the analysis of internal K content. These V_K values from our IRK1 experiments were similar to but somewhat more depolarized than the mean value of -40 mV

we obtained under identical conditions with *Shaker* K channels (Stampe and Begenisich, 1996).

Since the computation of n' from Eq. 2 is inversely related to the difference between the test and K^+ equilibrium potential, measurement errors become increasingly important for test potentials near the equilibrium potential. Uninjected oocytes exhibited current $< 0.1 \mu\text{A}$ near -40 mV and so had a negligible effect on our measurement of the K equilibrium potential. However, to minimize errors that might result from the slightly more depolarized equilibrium potential of IRK1-injected oocytes, we included IRK1 flux measurements at -25 mV in addition to the -30-mV test voltage we used for *Shaker* channel experiments.

RESULTS

IRK1 Currents and Fluxes

Fig. 1 A shows examples of currents from an oocyte expressing IRK1 channels. The membrane voltage was maintained at +20 mV and pulsed (for 300 ms) to the potentials indicated. The currents in Fig. 1 B were measured at the end of the 300-ms pulses at the potentials of the abscissa. This strongly rectifying current-voltage

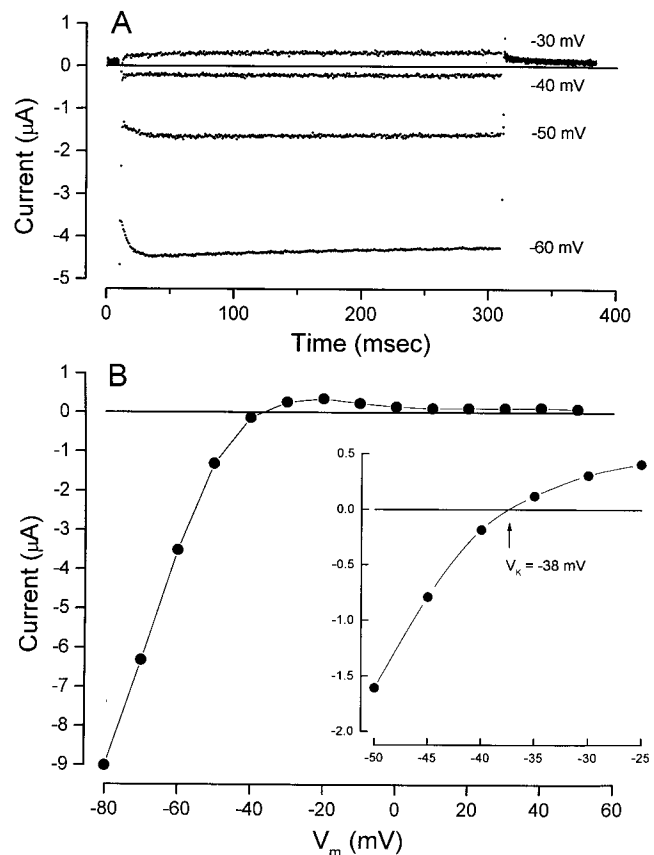


FIGURE 1. IRK1 K^+ channel currents during step hyperpolarizations. (A) Superimposed current records in response to 300-ms hyperpolarizations to -60, -50, -40, and -30 mV from a holding potential of +20 mV. (B) Currents at the end of the 300-ms pulses as a function of test potential. (inset) Current-voltage relation from the same oocyte obtained at potentials close to the zero current potential, V_K .

relation is expected for the IRK1 channel (Kubo et al., 1993). Fig. 1, *inset*, illustrates the method of determining V_K necessary for computation of the flux-ratio exponent (see Eq. 2). Currents were recorded at 5-mV intervals near the reversal potential and a second-order polynomial was fit to the data from which the V_K value was obtained (-38 mV in this case).

The unidirectional K influx was obtained by repetitively applying 300-ms pulses from a holding potential of $+20$ mV (see METHODS for details). The net flux was obtained by collecting all the associated current records and integrating these over the duration of the applied pulse. The unidirectional efflux was obtained from these two measurements (see Eq. 3) and, with the measured V_K value, the flux-ratio exponent, n' , was computed (Eq. 2). Fig. 2 summarizes n' values obtained at -50 , -30 , and -25 mV plotted as a function of the measured influx. Most values are near or between 2 and 3 and appear independent of membrane potential and influx value. This latter observation controls for any systematic error that might have been associated with measurements of small flux values.

Fig. 3, *inset*, illustrates an experiment designed to measure unidirectional K efflux. As described in METHODS, the amount of ^{42}K leaving the oocyte was collected at 1-min intervals in the tubes of a fraction collector. The inset represents the amount of ^{42}K in each sample converted to flux units. It is apparent that after a brief period during which the membrane was maintained at $+20$ mV, the efflux appears to reach a relatively constant value. The efflux increased substantially after a change of the holding potential to -25 mV and decreased to near baseline value when the potential was

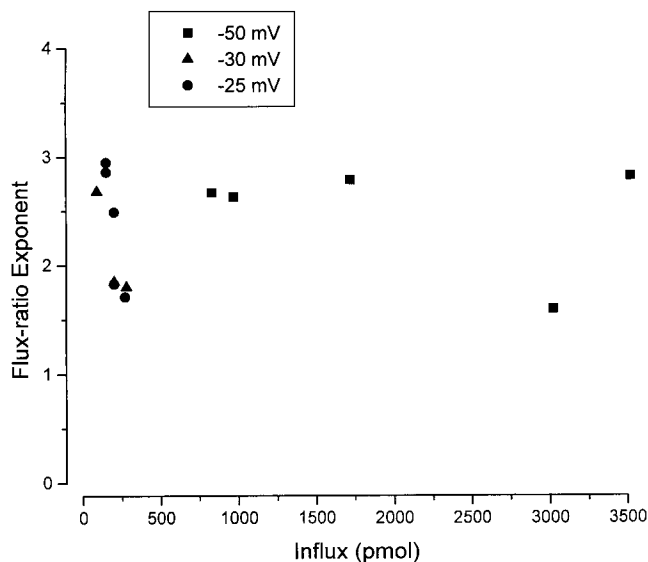


FIGURE 2. IRK1 channel flux-ratio exponent from influx experiments. Flux-ratio values at -50 (■), -30 (▲), and -25 (●) mV as a function of influx.

returned to $+20$ mV. The net current associated with the period at -25 mV was integrated to obtain the net flux and the influx computed by subtraction. As with the influx method, the K^+ equilibrium potential was measured, and the flux-ratio exponent computed.

Fig. 3 summarizes the flux-ratio exponent values obtained at -50 , -30 , and -25 mV (● and ■). We determined n' at -25 mV using both the influx and efflux methods and found quite similar values: 2.4 ± 0.26 ($n = 5$, ■) and 2.1 ± 0.21 ($n = 4$, ●) for the influx and efflux methods, respectively. Considering the very different sources of experimental errors associated with these two methods (Begenisich and De Weer, 1980; Stampe and Begenisich, 1996), the similarity of the results adds confidence to the values obtained. The n' values at -30 and at -50 mV were found to be 2.1 ± 0.29 (3) and 2.5 ± 0.23 (5), respectively.

Our intention was to compare the flux-ratio exponent values of IRK1 and *Shaker* K channels. The very different voltage range for activation of these two channel types constrains this comparison to voltages near -30 mV. The average value for *Shaker* channels at -30 mV is 3.4 ± 0.27 (7) (Stampe and Begenisich, 1996) and this value is included in Fig. 3 (Δ). As noted above, the value for IRK1 channels at -30 mV was 2.1, considerably smaller than that for *Shaker* channels. The number of successful IRK1 experiments at -30 mV was limited because many oocytes had V_K values rather close to this potential (see METHODS), which makes the computation of n very sensitive even to small errors in V_m or V_K . However, as can be seen in Fig. 3, the IRK1 flux-ratio exponent was quite insensitive to membrane potential over the range -50 to -25 mV with a value between 2.1 and 2.5.

The results presented in Fig. 3 show that the flux-ratio exponent values of IRK1 channels were considerably smaller than comparable values from *Shaker* K channels. As discussed below, such differences could reflect differences in the number of K^+ ion binding sites in the pores of these two channel types. Alternatively, the number of sites in each type of pore could be the same, but other properties of the pore may result in the manifestation of different n' values (Hille and Schwarz, 1978; see also Fig. 6). A useful method to probe other possible differences in the permeation pathway is to measure the single channel conductance as a function of the symmetrical concentration of K^+ flanking the pore (Hille and Schwarz, 1978).

IRK1 Single Channel Currents

Fig. 4 A contains single channel currents obtained from an excised inside-out patch of *Xenopus* oocyte membrane expressing an IRK1 channel in symmetrical 100 mM K^+ . From many such records at each potential, current histograms were constructed, and Fig. 4 B illus-

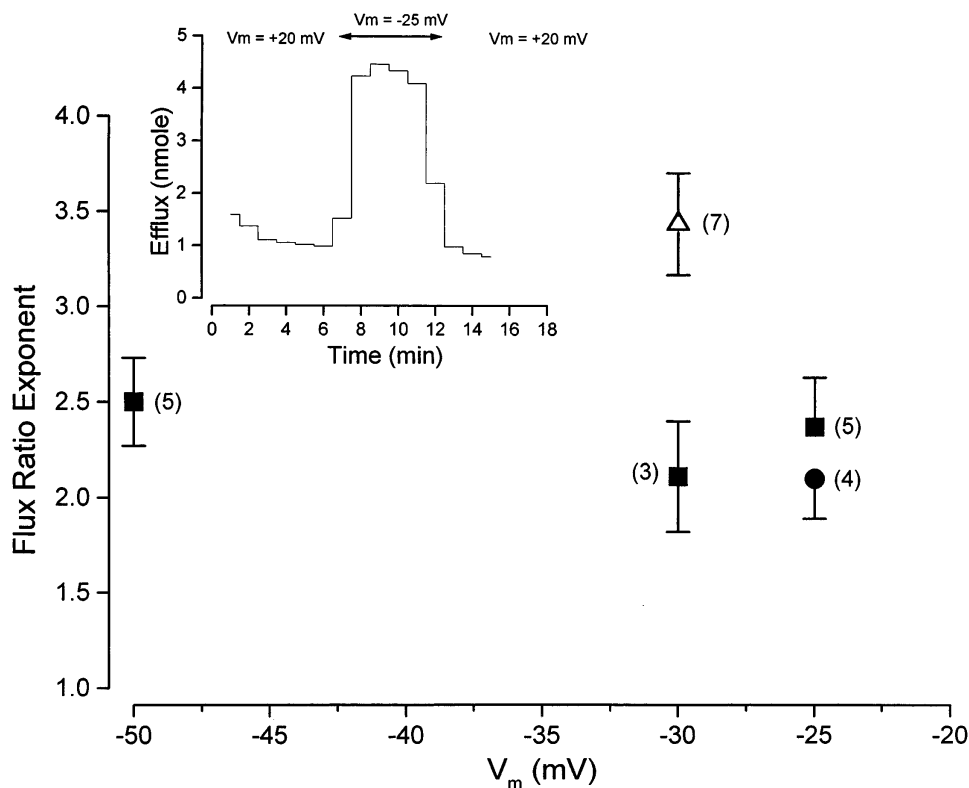


FIGURE 3. Flux-ratio exponent data from influx and efflux experiments. (*inset*) ^{42}K efflux determined as the number of counts in 1-min samples, corrected for radioactive background as described in METHODS. The oocyte membrane potential was maintained at +20 mV except for the indicated 4-min period when the potential was -25 mV. (*main figure*) Flux-ratio exponent values at several potentials. Shown are mean flux-ratio values with SEM limits from IRK1 channel influx measurements (■) at -50, -30, and -25 mV, and the mean value from efflux measurement at -25 mV (●). The mean of *Shaker* K channel flux-ratio values from both influx and efflux measurements (from Stampe and Begenisich, 1996) at -30 mV is shown (△) for comparison. The number of measurements are shown in parentheses.

trates an example for currents recorded at -80 mV from the same patch. Superimposed on the histogram is the fit of two Gaussian functions with the nonzero component reflecting a single channel current of -1.7 pA. The complete current-voltage relation for the channel in this patch is illustrated in Fig. 4 C. Most single channel current-voltage relations were relatively linear, but some, like the example in Fig. 4 C, were slightly inward rectifying (see Lopatin and Nichols, 1996, for similar examples). To obtain the zero-voltage slope conductance from even nonlinear current-voltage relations, a second-order polynomial was fit to the data. For the example in Fig. 4 C (*line*), a value of 19 pS was obtained.

Fig. 5 summarizes our single channel conductance data. For this figure, the K concentrations have been converted to ion activities with activity coefficients from Kielland (1937). The data can be fit by a saturating hyperbola (Fig. 5, *line*) with a maximum conductance of 32 pS and a half-maximal K activity of 40 mM.

Permeation Models

The process of ion permeation is quite complex, especially if, as appears to be the case for many types of ion channels, it involves simultaneous occupancy of the pore by two or more ions. Some insight into this process has been obtained by considering experimental data in some theoretical context, and reaction rate theory

(Glasstone et al., 1941) has been quite useful for this purpose (but see Eisenberg, 1996, and the discussion in Chen et al., 1997, for an alternative formalism). Hille and Schwarz (1978) described how the multi-ion properties of many types of K channel can be understood in terms of barrier models of permeation. We used this form of analysis to determine the general types of barrier models that could be consistent with the available data on K^+ permeation through IRK1 channels.

Since we found flux-ratio values for IRK1 channels between 2 and 3, a barrier model for such a pore must have at least three K ion binding sites. Consequently, we considered a model consisting of four barriers and three sites. Ions move in single file from site to empty site across the intervening energy barrier. The rate of movement decreases exponentially with the free-energy difference between the site and the intervening barrier, biased for membrane potential. We did not assume any repulsion between ions in the model as doing so would add another free parameter and would, for any given energy profile and ion concentration, have the effect of lowering the computed flux-ratio exponent (Hille and Schwarz, 1978). The mathematics and computations for this model were extended from the three-barrier, two-site model of Begenisich and Cahalan (1980a) and has been used to simulate some permeation properties of native (Begenisich and Smith, 1984) and expressed voltage-gated K channels (Pérez-Cornejo and Begenisich, 1994).

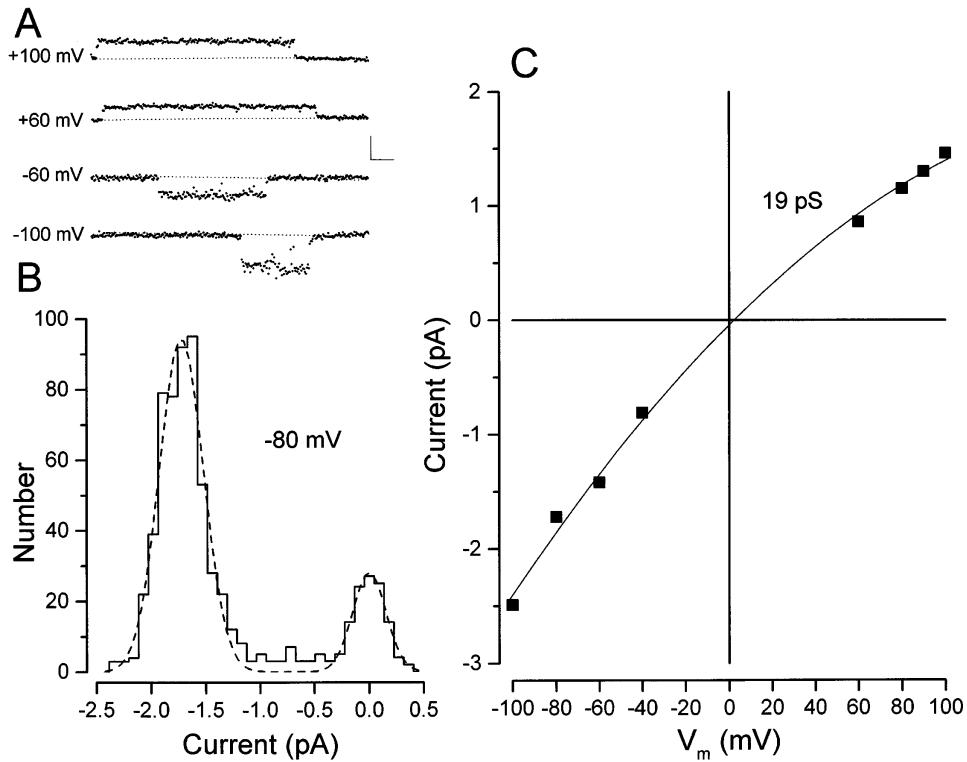


FIGURE 4. IRK1 single channel current. (A) Sample single channel current measurements at the indicated potentials recorded from an inside-out patch with symmetrical 100 mM K^+ solutions. The dotted line represents the zero current level for each record. Calibration: 2 pA and 50 ms. (B) Current amplitude histogram from several records from the same patch obtained at -80 mV. (line) A two-Gaussian function fitted to the data. The non-zero component is centered on a level of -1.7 pA. (C) Single channel currents from the same patch at several potentials. (line) Fit of a second-order polynomial to the data from which a zero-current slope of 19 pS was obtained.

Fig. 6 contains simulations of some permeation properties for several classes of a model with the energy barrier profiles illustrated at the top ($1 RT = 0.58$ kcal/mol). Shown are the computed single channel current-voltage relation, conductance activity, and voltage dependence of the flux-ratio exponent (Fig. 6, *top* to *bottom*, respectively).

The ion energy barrier profile for the model in Fig. 6 (*left*) is dominated by a single large barrier. This model predicts (*dashed line*) an outwardly rectifying current-voltage relation with a symmetrical ion activity of 50 mM. The solid line represents the current-voltage relation for a 200-mM symmetrical solution. The predicted conductance-activity relation for this barrier profile reaches a maximum near 150 mM, and then decreases. Lastly, even though this is a three-ion pore, the predicted flux-ratio exponent is 1.0 over the voltage range from -100 to 100 mV. The shape of the current-voltage relation is sensitive to the location of the largest barrier (Begenisich and Cahalan, 1980*b*). The activity at which the peak conductance occurs is less sensitive to barrier position (Hille and Schwarz, 1978). The flux-ratio exponent value is quite insensitive to the position of the rate-limiting barrier and is negligibly larger than 1.0. Thus, this class of permeation barrier models is inconsistent with the IRK1 permeation data, especially the flux-ratio exponent data of Fig. 3.

Hille and Schwarz (1978) noted that, for a barrier model to exhibit a flux-ratio exponent that approaches

the number of ion binding sites, the lateral barriers need to be significantly larger than the interior barriers. This arrangement enhances several multi-ion permeation properties by maximizing the likelihood that

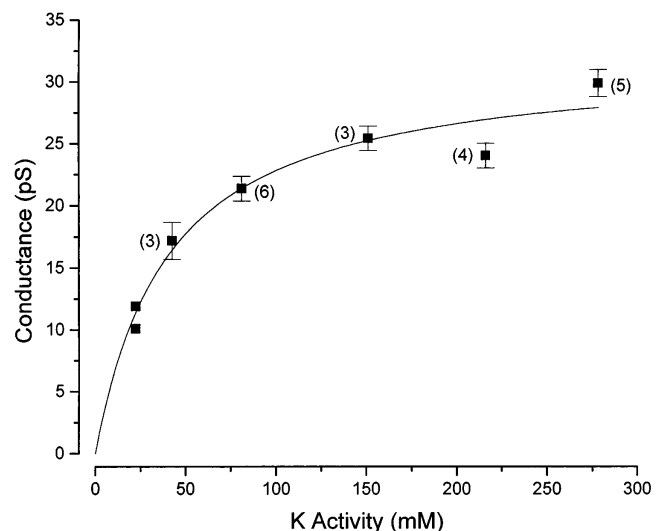


FIGURE 5. IRK1 single channel conductance as a function of symmetrical K^+ activity. Mean single channel conductance level and standard error limits are shown. The number of patches is shown in parentheses, except at the lowest K activity, where the two symbols represent individual patches. (line) A rectangular hyperbola fit to the data with a maximum of 32 pS and a half-maximal activity of 40 mM.

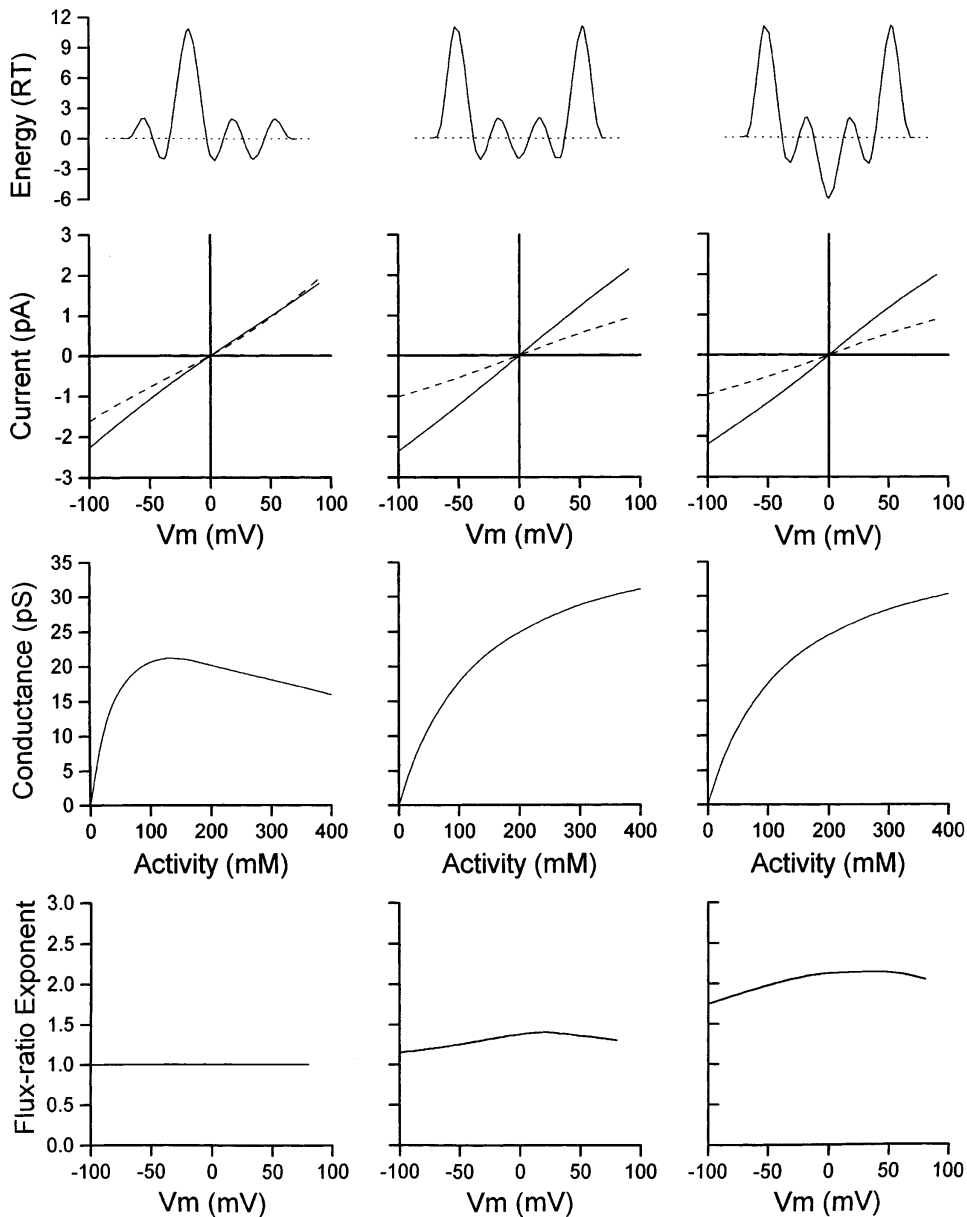


FIGURE 6. Permeation properties and barrier profiles. Each column represents a different permeation model characterized by the zero-voltage free energy barrier profile at the top. In all cases, the energy minima and maxima are equally spaced along the membrane electric field. The external solution is to the left of the barriers. Below the barrier profile in each column are the computed current-voltage relations at 50 (*dashed line*) and 200 (*solid line*) mM symmetrical ion concentration, the ion activity dependence of the zero-voltage slope conductance, and the flux-ratio exponent over the -100 - to 100 -mV voltage range.

occupancy vacancies are filled by ions within the pore rather than by a new ion entering it. The energy barrier profile in Fig. 6 (*middle*) is the three-site extension of one of those analyzed by Hille and Schwarz (1978). This model reproduces the near linear IRK1 single channel current-voltage relations as well as the experimental conductance-activity relation. The flux-ratio exponent of this model has a maximum value near 1.4, significantly less than our measured values. For this general type of barrier profile, the flux-ratio exponent can be increased to near 1.8 by increasing the depth of the three energy wells by only 1 *RT*. However, doing so significantly reduces the single channel current (and conductance) and causes the conductance-activity relation to saturate at very low K concentrations (not shown).

Fig. 6 (*right*) contains the predictions of a simple alteration in the middle barrier profile, making only the central well deeper. This modification increases the flux-ratio exponent to values near 2.2, in close agreement with our experimental results, but preserves single-channel current voltage and conductance saturation relations, consistent with the experimental data. Thus, a three-site pore with an energy profile consisting of high lateral, low internal barriers, and a deep central well is quite consistent with the fundamental permeation properties of IRK1 channels.

DISCUSSION

We measured unidirectional K^+ fluxes through IRK1 channels expressed in *Xenopus* oocytes. In each experi-

ment, we measured net flux (ion current) and either unidirectional influx or efflux. The remaining unidirectional flux was computed from the measured flux and net current (see METHODS). With these unidirectional fluxes, we determined the flux-ratio exponent, n' (Eq. 2), which had values between 2 and 2.5 over the voltage range from -50 to -25 mV. The flux-ratio was determined at -25 mV in experiments in which unidirectional influx was measured and in experiments in which efflux was directly measured. These two types of experiments yielded results that did not significantly differ from one another ($P = 0.5$), with an overall mean n' value of 2.3 ± 0.16 (9).

Northern blot analysis indicates that mRNA coding for IRK1 channels is present at high concentrations in skeletal muscle (Kubo et al., 1993) and the inward rectifier K channels expressed in this tissue are likely comprised, in large part, of IRK1 protein. Unidirectional K^+ fluxes across the surface membrane of skeletal muscle have been measured and the flux-ratio exponent determined (Horowicz et al., 1968; Spalding et al., 1981). At low external K concentrations, the flux-ratio exponent was found to be near 1.0, and near 2 for high concentrations. In spite of very different experimental conditions, our results are in general agreement with the latter value.

The experimental conditions used here were identical to those used to determine n' values for *Shaker* K channels (Stampe and Begenisich, 1996), and so a direct comparison between results from these two channel types is possible. At -30 mV, *Shaker* channels exhibit an n' value of 3.4 ± 0.27 (7), significantly larger than the IRK1 values at -30 and -25 mV of 2.1 ± 0.29 (3) and 2.3 ± 0.16 (9), respectively.

We determined IRK1 single channel slope conductance (at 0 mV) as a function of symmetrical K^+ concentration in the absence of Mg^{2+} , and polyamines that produce the inward rectification of this channel (Lopatin et al., 1994; Ficker et al., 1994). Our results are quite similar to data obtained in symmetrical 100- and 140-mM K^+ solutions by Aleksandrov et al. (1996) and Ficker et al. (1994), respectively. We found that the conductance–activity relation could be described by a saturating hyperbola with a half-saturation K^+ activity of 40 mM and a predicted maximum of 32 pS.

The conductance–concentration relation of IRK1 channels determined in this study was generally similar to the behavior of the weak inward rectifier channel, ROMK1, for K^+ concentrations as large as 400 mM (Lu and MacKinnon, 1994). At larger K concentrations, the conductance of single ROMK1 channels decreases, another manifestation of multi-ion pores (Lu and MacKinnon, 1994; Hille and Schwarz, 1978).

The dependence of the conductance of voltage-gated K channels on K^+ concentration is quite different than

the inward rectifier channels ROMK1 and IRK1. The conductance of single *Shaker* K channels reaches a maximum near a K^+ activity of 1 M with a half-maximal concentration near 300 mM (Heginbotham and MacKinnon, 1993), which is quite similar to the behavior of the macroscopic conductance of voltage-gated K channels in the squid giant axon (Wagoner and Oxford, 1987).

A variety of theoretical approaches have been used to provide an interpretation of flux-ratio exponent values >1.0 (e.g., Hodgkin and Keynes, 1955; Heckmann, 1972; Hille and Schwarz, 1978; see references in Levitt, 1986; Schumaker, 1992; Bek and Jakobsson, 1994). In spite of the mathematical formalism used, the same conclusion is reached: only permeation models that allow multiple ion occupancy of the pore predict flux-ratio exponent values >1.0 . In all these calculations (except for one limiting case, Hodgkin and Keynes, 1955), the flux-ratio exponent may approach, but cannot exceed, the number of ions that can simultaneously occupy the pore. For any particular model parameters, the flux-ratio exponent may be much less than the maximum (e.g., see Fig. 6). Thus, the flux-ratio exponent provides an estimate of the minimum number of ions that may occupy the pore. Our results show that the pore in IRK1 channels is capable of containing at least three K^+ ions.

We showed that a relatively simple four-barrier, three-site permeation model can quantitatively account for the flux-ratio and conductance–activity data and qualitatively for the current–voltage relations. Since our goal was to examine some general classes of such models, we made no effort to adjust the model parameters to quantitatively reproduce the current–voltage data. Nevertheless, this exercise revealed that the presence of a deep central well is a key feature for enhancing the magnitude of the predicted flux-ratio exponent. This same feature was found useful in describing ion selectivity in Ca^{2+} channels (Dang and McClesky, 1998) and in describing the interactions of Na^+ and K^+ ions in some types of voltage-gated K channels (Kiss et al., 1998). While far from confirming the existence of a dominant high affinity binding site for permeant ions, the convergence of several investigations toward a similar conclusion suggests that it may be worthwhile to design experimental tests of this idea.

Conclusion

As discussed above, the flux-ratio exponent does not directly determine the number of ions that may occupy the pore. Rather, it establishes only the minimum number of ions that may do so. Thus, the different n' values for *Shaker* and IRK1 channels could each be consistent with a pore that could simultaneously be occupied by four (or more) ions. Furthermore, Lu and MacKinnon

(1994) showed that the difference between the ROMK1 and *Shaker* conductance–concentration relations could result simply from a change in ion entry rates in one type of permeation model. Thus, establishing the maximum occupancy of a pore requires other data.

A Rb⁺ Fourier difference map of a prokaryotic K channel (KcsA) shows that in 150 mM RbCl this channel is occupied by three Rb⁺ ions (Doyle et al., 1998). Two of these are within ~ 7.5 Å of each other, at the ends of the highly conserved selectivity filter sequence (TVGYG; Heginbotham et al., 1994) in the channel pore region. K⁺ ions may occupy similar sites since Rb⁺ and K⁺ share much physical similarity and have generally similar permeation properties. The KcsA channel is structurally similar to IRK1 in having two membrane spanning domains and the K channel selectivity filter sequence. So even though the other amino acids in the KcsA pore region are much more similar to *Shaker* than to IRK1 channels, the simplest picture of inward rectifier K channels consistent with all the permeation data is that these channels have three sites that may all be si-

multaneously occupied. We showed that the flux-ratio and permeation data for IRK1 channels can be simulated by at least one class of three-site permeation models.

As noted above, the flux-ratio exponent for *Shaker* K channels is near 3.5, much larger than that determined for inward rectifier channels. This result and the results of a study of Ba²⁺ block of Ca²⁺-activated K channels (Neyton and Miler, 1988) indicates that some classes of K channels can accommodate at least four K⁺ ions. Thus, the structural picture of Rb⁺ ion occupancy of the KcsA may not apply to K⁺ ion occupancy of all classes of K channels. Either KcsA channels can be occupied by more K⁺ than Rb⁺ ions or (more likely) there may be ion coordinating structures in voltage-gated K channels not represented in KcsA (or inward rectifier) channels. Candidates for additional K⁺ binding sites may include regions in S6 and the S4–S5 linker since mutations in these areas alter K channel permeation properties (Isacoff et al., 1991; Choi et al., 1993; Slesinger et al., 1993; Lopez et al., 1994).

We are grateful to L.Y. Jan for providing the IRK1 cDNA and to Jay Yang for the high expression *Xenopus* vector. We thank Jill Thompson for technical assistance with the experiments and for critically reading the manuscript.

This work was supported in part by National Science Foundation grant IBN-9514389 (T. Begenisich).

Original version received 16 April 1998 and accepted version received 3 August 1998.

REFERENCES

- Aleksandrov, A., B. Velimirovic, and D.E. Clapham. 1996. Inward rectification of the IRK1 K⁺ channel reconstituted in lipid bilayers. *Biophys. J.* 70:2680–2687.
- Begenisich, T., and M.D. Cahalan. 1980a. Sodium channel permeation in squid axons. I: Reversal potential experiments. *J. Physiol. (Camb.)*. 307:217–242.
- Begenisich, T., and M.D. Cahalan. 1980b. Sodium channel permeation in squid axons. II: Non-independence and current–voltage relations. *J. Physiol. (Camb.)*. 307:217–242.
- Begenisich, T., and P. De Weer. 1980. Potassium flux ratio in voltage clamped squid giant axons. *J. Gen. Physiol.* 76:83–98.
- Begenisich, T., and C. Smith. 1984. The multi-ion nature of potassium channels in squid axons. In *Current Topics in Membranes and Transport*. Vol. 22. The Squid Axon. P.F. Baker, editor. Academic Press Inc., New York. 353–369.
- Bek, S., and E. Jacobsson. 1994. Brownian dynamics study of a multiply-occupied cation channel: application to understanding permeation in potassium channels. *Biophys. J.* 66:1028–1038.
- Chen, D., J. Lear, and B. Eisenberg. 1997. Permeation through an open channel: Poisson-Nernst-Planck theory of a synthetic ionic channel. *Biophys. J.* 72:97–116.
- Choi, K.L., C. Mossman, C. Aube, and G. Yellen. 1993. The internal quaternary ammonium receptor site of *Shaker* potassium channels. *Neuron*. 10:533–541.
- Dang, T.X., and E.W. McCleskey. 1998. Ion channel selectivity through stepwise changes in binding affinity. *J. Gen. Physiol.* 111:185–193.
- Doyle, D.A., J.M. Cabral, R.A. Pfuetzner, A. Kuo, J.M. Gulbis, S.L. Cohen, B.T. Chait, and R. MacKinnon. 1998. The structure of the potassium channel: molecular basis of K⁺ conduction and selectivity. *Science*. 280:69–77.
- Eisenberg, R.S. 1996. Computing the field in proteins and channels. *J. Membr. Biol.* 150:1–25.
- Ficker, E., M. Taglialatela, B.A. Wible, C.M. Henley, and A.M. Brown. 1994. Spermine and spermidine as gating molecules for inward rectifier K⁺ channels. *Science*. 266:1068–1072.
- Glasstone, S., K.J. Laidler, and H. Eyring. 1941. The theory of rate processes. McGraw-Hill, New York. 611 pp.
- Goldin, A.L. 1992. Maintenance of *Xenopus laevis* and oocyte injection. *Methods Enzymol.* 207:266–279.
- Heckmann, K. 1972. Single file diffusion. *Biomembranes*. 3:127–153.
- Heginbotham, L., Z. Lu, T. Abramson, and R. MacKinnon. 1994. Mutations in the K⁺ channel signature sequence. *Biophys. J.* 66:1061–1067.
- Heginbotham, L., and R. MacKinnon. 1993. Conduction properties of the cloned *Shaker* K⁺ channel. *Biophys. J.* 65:2089–2096.
- Hille, B., and W. Schwarz. 1978. Potassium channels as multi-ion single-file pores. *J. Gen. Physiol.* 72:409–442.
- Hodgkin, A.L., and R.D. Keynes. 1955. The potassium permeability of a giant nerve fibre. *J. Physiol. (Camb.)*. 128:61–88.
- Horowicz, P., P.W. Gage, and R.S. Eisenberg. 1968. The role of electrochemical gradient in determining potassium fluxes in frog striated muscle. *J. Gen. Physiol.* 51:193s–203s.
- Isacoff, E., Y.N. Jan, and L.Y. Jan. 1991. Putative receptor for the cy-

- toplasmic inactivation gate in the *Shaker* K⁺ channel. *Nature*. 353: 86–90.
- Kielland, J. 1937. Individual activity coefficients of ions in aqueous solutions. *J. Am. Chem. Soc.* 59:1657–1678.
- Kiss, L., D. Immke, J. LoTurco, and S.J. Korn. 1998. The interaction of Na and K in voltage-gated potassium channels. Evidence for cation binding sites of different affinity. *J. Gen. Physiol.* 111:195–206.
- Kubo, Y., T.J. Baldwin, Y.N. Jan, and L.Y. Jan. 1993. Primary structure and functional expression of a mouse inward rectifier potassium channel. *Nature*. 362:127–133.
- Lu, Z., and R. MacKinnon. 1994. A conductance maximum observed in an inward-rectifier potassium channel. *J. Gen. Physiol.* 104:477–486.
- Levitt, D.G. 1986. Interpretation of biological ion channel flux data: reaction-rate versus continuum theory. *Annu. Rev. Biophys. Biophys. Chem.* 15:29–57.
- Lopatin, A.N., and C.G. Nichols. 1996. [K⁺] dependence of open-channel conductance of cloned inward rectifier potassium channels (IRK1, Kir2.1). *Biophys. J.* 71:682–694.
- Lopatin, A.N., E.N. Makhina, and C.G. Nichols. 1994. Potassium channel block by cytoplasmic polyamines as the mechanism of intrinsic rectification. *Nature*. 372:366–369.
- Lopez, G.A., Y.N. Jan, and L.Y. Jan. 1994. Evidence that the S6 segment of the *Shaker* voltage-gated K⁺ channel comprises part of the pore. *Nature*. 367:179–182.
- Neyton, J., and C. Miller. 1988. Discrete Ba²⁺ block as a probe of ion occupancy and pore structure in the high-conductance Ca²⁺-activated K⁺ channel. *J. Gen. Physiol.* 92:569–586.
- Pérez-Cornejo, P., and T. Begenisich. 1994. The multi-ion nature of the pore in *Shaker* K⁺ channels. *Biophys. J.* 66:1929–1938.
- Schumaker, M.F. 1992. Shaking stack model of ion conduction through the Ca²⁺-activated K⁺ channel. *Biophys. J.* 63:1032–1044.
- Slesinger, P.A., Y.N. Jan, and L.Y. Jan. 1993. The S4–S5 loop contributes to the ion-selective pore of potassium channels. *Neuron*. 11:739–749.
- Spalding, B.C., O. Senyk, J.G. Swift, and P. Horowicz. 1981. Unidirectional flux ratio for potassium ions in depolarized frog skeletal muscle. *Am. J. Physiol.* 241:68–75.
- Stampe, P., and T. Begenisich. 1996. Unidirectional K fluxes through recombinant *Shaker* potassium channels expressed in single *Xenopus* oocytes. *J. Gen. Physiol.* 107:449–457.
- Stampe, P., and T. Begenisich. 1998. Unidirectional fluxes through ion channels expressed in *Xenopus* oocytes. *Methods Enzymol.* 293: 556–564.
- Ussing, H.H. 1949. The distinction by means of tracers between active transport and diffusion. The transfer of iodide across the isolated frog skin. *Acta Physiol. Scand.* 19:43–56.
- Vestergaard-Bogind, B., P. Stampe, and P. Christophersen. 1985. Single-file diffusion through the Ca²⁺-activated K⁺ channel of human red cells. *J. Membr. Biol.* 88:67–75.
- Wagoner, K.P., and G.S. Oxford. 1987. Cation permeation through the voltage-dependent potassium channel in the squid axon. Characteristics and Mechanisms. *J. Gen. Physiol.* 90:261–290.
- Yang, J., Y.N. Jan, and L.Y. Jan. 1995. Control of permeation by residues in two distinct domains in an inward rectifier K⁺ channel. *Neuron*. 14:1047–1054.